Letter

Observation of direct hole Rashba spin-orbit coupling in *p*-type GaAsSb nanowires

Zhenhao Sun,[1,*] Shuaiyu Chen,[1,*] Ning Tang,[1,3,5,†] Dong Pan,[2] Hongming Guan,[1] Xiaoyue Zhang,[1] Shixiong Zhang,[1] Jianhua Zhao,[2,4] Jun-Wei Luo,[2,4,‡] Shu-Shen Li,[2] Weikun Ge,[1] and Bo Shen[1,3,5]

[1]*State Key Laboratory of Artificial Microstructure and Mesoscopic Physics, School of Physics, Peking University, Beijing 100871, China*

[2]*State Key Laboratory of Superlattices and Microstructures, Institute of Semiconductors, Chinese Academy of Sciences, Beijing 100083, China*

[3]*Frontiers Science Center for Nano-optoelectronics & Collaboration Innovation Center of Quantum Matter, Peking University, Beijing 100871, China*

[4]*Beijing Academy of Quantum Information Sciences, Beijing 100193, China*

[5]*Peking University Yangtze Delta Institute of Optoelectronics, Nantong 226010, Jiangsu, China*

(Received 11 May 2023; revised 31 July 2023; accepted 3 August 2023; published 18 August 2023)

A strong linear-in-*k* Rashba spin-orbit coupling (SOC) has been discovered theoretically for holes in semiconductor nanowires originating from direct dipolar coupling to the external electric field. Such direct Rashba SOC effect not only overcomes the major drawback of the hole Rashba SOC for its leading order being cubic-in-*k* but also renders its strength orders of magnitude stronger than the corresponding electron counterpart. Here, the direct hole Rashba SOC effect has been experimentally observed through the circular photogalvanic effect (CPGE) by conducting the experimental measurement of a helicity-dependent photocurrent in the *p*-type $GaAs_{1-x}Sb_x$ semiconducting nanowires upon application of an external gate voltage at room temperature. We have observed that the CPGE current undergoes a transition from rapid increase to saturation as the gate voltage varies. This finding is consistent with the predicted common feature of the direct Rashba SOC of holes in semiconductor nanowires, providing clear evidence for the theoretical concept.

DOI: 10.1103/PhysRevB.108.L081302

Because of the spin-momentum locking effect, the spin-orbit coupling (SOC) plays a crucial role in diverse fields of condensed-matter physics, including the investigation of Majorana fermions, topological insulators, quantum information, and spintronics [1–10]. Specifically, the Rashba SOC effect is electrically tunable and locks the spin orientation perpendicular to the electron momentum. These features are decisive towards robust semiconductor-based spintronic devices in which spin polarization is generated from charge current, manipulated by electric fields and detected as voltage [11–15]. Therefore, a strong and tunable Rashba SOC effect is crucial for the implementation of spintronic functions [16,17]. However, the Rashba SOC of electrons in conventional III-V and group IV semiconductors is much weaker than required [18], which has stimulated search of a strong Rashba effect in novel semiconductors or low-dimensional semiconductor structures [19–23]. Moreover, the nuclear hyperfine interactions enforced by nuclear spins lead to a short coherence lifetime of electron spins in quantum confined system [18,22,23]. In contrast, the top valence bands steaming from atomic *p* orbitals in semiconductors make holes weak coupling to nuclear spins. Therefore, holes possess the potential for longer coherence spin lifetimes [22,23]. However, holes mainly in the heavy-hole band have a critical drawback for spintronic applications considering the fact that its dominant *k*-cubic Rashba effect is very weak in contrast to its *k*-linear electron counterpart [24,25].

Fortunately, this drawback of holes has been overcome by the discovery of a strong linear-in-*k* hole Rashba SOC effect in semiconductor nanowires, which arises from the direct dipolar coupling to the external electric field [26–28]. This direct hole Rashba SOC is a first-order effect with orders of magnitude stronger than the third-order conventional hole Rashba SOC in 2D systems [26]. For example, the saturated magnitude of the hole Rashba SOC in Si nanowires is enhanced by a factor of 2000 in comparison with its electron counterpart and achieves 100 meVÅ, which exceeds the reported record of the electron Rashba effect in narrow band-gap InAs heterostructures [26,27]. This direct Rashba SOC has a signature of sharp rising and then becoming saturation in strength upon application of an external electric field, which is essential for practical application under low electric field and the device robustness against fluctuations in an applied electric field [27]. Hence, a clear experimental signature of this direct hole Rashba SOC is important to evidence the theoretical calculation [27].

In this Letter, we take *p*-type direct band-gap $GaAs_{1-x}Sb_x$ nanowires with different Sb contents and wire sizes to study the Rashba SOC of holes in semiconductor nanowires utilizing the circular photogalvanic effect (CPGE) at room temperature. We demonstrated that the CPGE photocurrent changes from a sharp increase to saturation with increasing magnitude of the applied external electric field. This change indicates a transition of the strength of the Rashba SOC

*Z.S. and S.C contributed equally to this work.
†ntang@pku.edu.cn
‡jwluo@semi.ac.cn

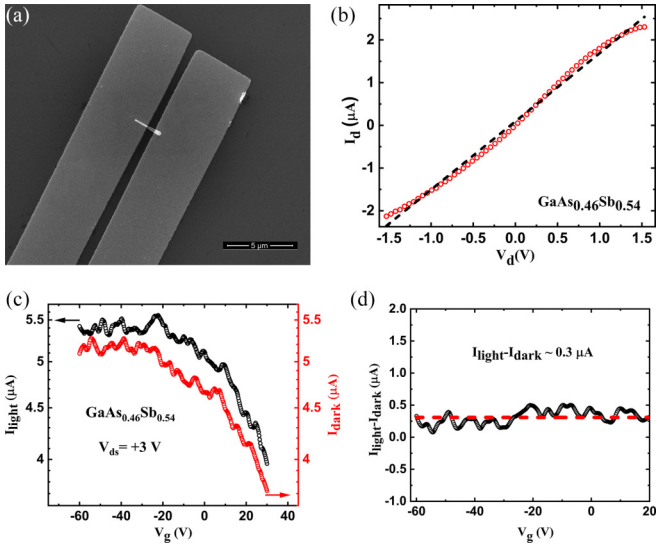

FIG. 1. Characterizations of $GaAs_{1-x}Sb_x$ nanowire device. (a) SEM image of $GaAs_{0.46}Sb_{0.54}$ nanowire device. Scale bar is 5 μm. (b) Current-voltage (I-V) curve of $GaAs_{0.46}Sb_{0.54}$ nanowire. (c) Transfer curve of $GaAs_{0.46}Sb_{0.54}$ nanowire with and without 635-nm laser shining on device. (d) Difference of transfer curve with and without illumination for $GaAs_{0.46}Sb_{0.54}$ device.

from field dependence to saturation regarding that the CPGE photocurrent is proportional to the Rashba SOC strength. This observation is consistent with the prediction presented in Ref. [27], and represents an experimental signature of the direct hole Rashba SOC.

The $GaAs_{1-x}Sb_x$ nanowires under investigation in this work were Ga self-catalyzed grown on Si (111) substrate by molecular-beam epitaxy, as shown in our previous paper [29]. These $GaAs_{1-x}Sb_x$ nanowires are in a pure zinc-blende crystal structure with the growth direction along [111] crystal orientation, as observed from the transmission electron microscopy measurements [29]. The sample contains a series of direct band-gap $GaAs_{1-x}Sb_x$ nanowires with a tunable Sb content-dependent band gap, together with an Sb content-dependent diameter. Here, two $GaAs_{1-x}Sb_x$ nanowires with $x = 0.18$ and $x = 0.54$ are chosen for the measurements, respectively. Their wire sizes are 75 and 225 nm in diameter with band gaps of 1.20 and 0.85 eV, respectively, as obtained from the photoluminescence spectra presented in Ref. [29]. To measure the electrical and optical properties, we transfer the as-grown $GaAs_{1-x}Sb_x$ nanowires onto a Si/SiO_2 substrate, followed by standard electron-beam lithography and e-beam evaporations of Cr/Au (20/80 nm) to fabricate the backgated devices. Figure 1(a) show the scanning electron microscopic (SEM) image of a fabricated $GaAs_{0.46}Sb_{0.54}$ nanowire device with corresponding current-voltage (I–V) curves exhibited in Fig. 1(b). The nanowire device exhibits an Ohmic contact behavior, eliminating the effect of Schottky contact on photocurrent measurements. The transfer curves of the nanowire device with and without 635-nm solid-state laser illumination are presented in Fig. 1(c). Obviously, the nanowire device manifests a p-type electrical conductivity according to the transfer curves, thus rendering the $GaAs_{1-x}Sb_x$ nanowires good candidates for studying the Rashba SOC of holes. Meanwhile, the difference of the transfer curve with and without illumination for the $GaAs_{0.46}Sb_{0.54}$ device has been obtained as shown in Fig. 1(d). It is worth noting that the independence of the photoinduced carrier conductivity from the gate voltage ensures the accuracy of the extracted Rashba SOC parameters in the following CPGE experiments.

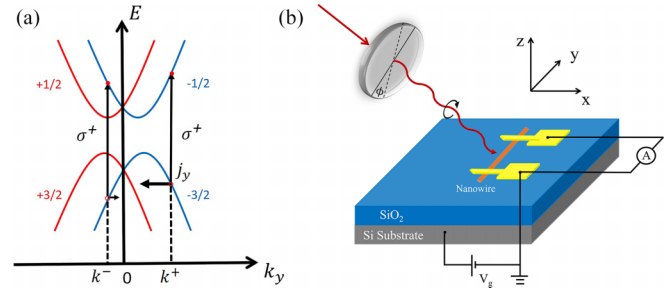

FIG. 2. (a) Diagram of CPGE current caused by band spin splitting induced by right-handed circularly polarized light, exciting valence electrons to conduction band. (b) Schematic of photocurrent measurement. Laser is in x-z plane and photocurrent is collected in y direction.

CPGE has been proven to be a sensitive and straightforward way to investigate the SOC and other spin-related phenomena [30–37]. As sketched in Fig. 2(a), under the premise of the k-linear spin splitting, the interband transition crossing the band gap excited by a circularly polarized light will generate asymmetric momentum distributions of electrons and/or holes along a special direction in the real space. This asymmetric distribution results in a net spin-polarized current (named as CPGE current) even without application of an external bias [30]. Generally, CPGE is closely associated with the spin splitting, and the amplitude of the CPGE current has a linear relationship with the SOC strength, which is quantified by the Rashba parameter. As the Rashba parameter can be manipulated by an external electric field, the magnitude of the CPGE current was found to be in proportion to the gate voltage and hence the Rashba parameter, as illustrated in our previous work [37]. Therefore, CPGE is a useful technique for studying the hole Rashba effect in p-type semiconducting nanowires. By measuring the CPGE current as a function of the gate voltage, we can further get the knowledge of the relationship between the Rashba parameter and applied external electric field. Figure 2(b) shows the schematic diagram of the CPGE measurement setup, where the incident laser passing through the quarter-wave plate irradiates onto the device, and the corresponding photocurrent is collected with a lock-in technique. According to the microscopic theory of CPGE, the CPGE current is linearly dependent on the SOC parameter α as [30]

$$J_{\mathrm{CPGE}} \propto n\alpha\eta\tau \sin\theta \sin 2\varphi, \tag{1}$$

where n is the density of the photon-induced carriers, η is the CPGE optical transition index, τ is the momentum relaxation time, θ is the incident angle of the light with respect to the surface normal, and φ is the rotation angle of the quarter-wave plate. The rotation of the quarter-wave plate provides a means to alter the helicity of the incident light. To distinguish the CPGE effect from other contributions, we measure

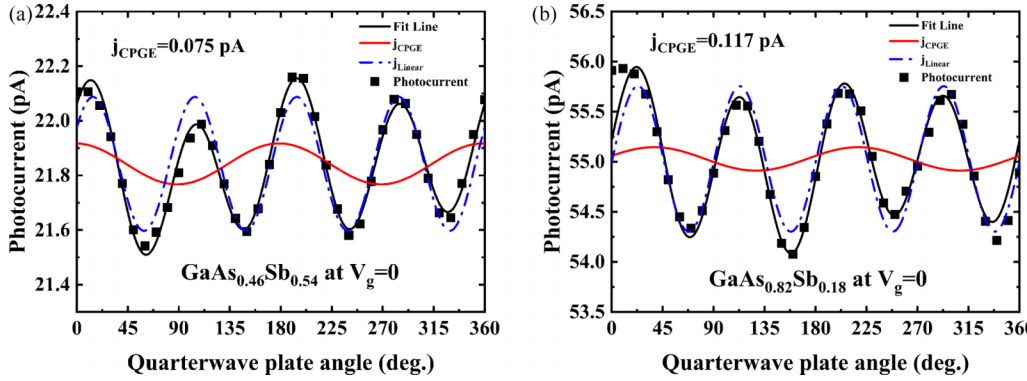

FIG. 3. Helicity-dependent photocurrent measurements of $GaAs_{0.46}Sb_{0.54}$ (a) and $GaAs_{0.82}Sb_{0.18}$ (b) nanowires without gate. CPGE can be observed in both nanowire devices. Black line is fitting line, while red lines and blue dashed lines represent CPGE and J_{linear} signals, respectively. Both CPGE and J_{linear} have been added with background J_0 for clarity.

the helicity-dependent photocurrent by rotating continuously the quarter-wave plate to tune the helicity of the incident light in covering the whole 2π period. The obtained helicity-dependent photocurrent is then fitted to the following equation [30]

$$J_{\text{photocurrent}} \propto C \sin 2\varphi + L_1 \sin 4\varphi + L_2 \cos 4\varphi + J_0. \quad (2)$$

In Eq. (2), the first term $J_{\text{CPGE}} = C \sin 2\varphi$ corresponds to the CPGE current having a π-periodic oscillation. The second term $J_{\text{LPGE}} = L_1 \sin 4\varphi$ represents the linear photogalvanic effect (LPGE) current with a $\frac{\pi}{2}$-periodic oscillation, resulting from asymmetric scattering of electrons. The third term $J_{\text{LPDE}} = L_2 \cos 4\varphi$ stands for the linear photon drag effect (LPDE) as a result of the momentum transfer from photons to carriers, which is also with a $\frac{\pi}{2}$-periodic oscillation. The final term J_0 accounts for the helicity-independent background photocurrent, which arises primarily from the photovoltaic effect at contacts, thermal effect, or Dember effect [30]. C, L_1 and L_2 are adjustable parameters representing the amplitudes of the CPGE, LPGE, and LPDE current, respectively. Here, only the CPGE current $J_{\text{CPGE}} = C \sin 2\varphi$ is relevant, since the LPGE, LPDE, and background currents have nothing to do with spin-related properties.

Given the p-type conducting nature of the GaAsSb nanowire devices, the photon-induced excess electrons are much more vulnerable to recombine than holes [38]. Thus, the photon-induced excess holes would be the primary carriers responsible for the photoconductivity. In such a situation, we could investigate the hole Rashba effect through CPGE. Figures 3(a) and 3(b) show the obtained helicity-dependent photocurrent from the $GaAs_{0.46}Sb_{0.54}$ and $GaAs_{0.82}Sb_{0.18}$ nanowire devices under zero gate voltage with application of a 635-nm solid-state laser serving as the excitation source. Fitting the obtained photocurrent to Eq. (2), we get CPGE signals in both nanowires, revealing the existence of the spin splitting in the valence bands even without applying an external gate voltage. We have demonstrated that the Dresselhaus SOC induced by the bulk-inversion asymmetry is absent in [111]-oriented GaAsSb nanowires with the crystal structure of the C_{3v} point group [28]. Subsequently, the above-observed CPGE (in the absence of external gate voltage) should stem exclusively from the Rashba SOC, which is induced by the structure-inversion asymmetry that occurred at the nanowire surface. Such structure-inversion asymmetry could arise from alloy atom distribution and most probably from the substrate, which gives rise to the surface band bending and the carriers' accumulation. Therefore, even without application of the external gate voltage, we can still observe a Rashba SOC-induced finite CPGE photocurrent for the existence of a surface-related external electric field.

We next manipulate the external electric field to investigate the Rashba effect for holes through examining the relationship between the CPGE current and external gate voltage. As a prerequisite, we have to take some necessary steps to eliminate other contributions to the CPGE current induced by the gate. According to Eq. (1), the amplitude of CPGE is not only in proportion to the hole Rashba SOC, but also the pure electrical parameters of photoinduced holes such as τ and n. In order to get rid of the pure electrical influences of photoinduced carriers during the participation of gate voltage, the transfer curves are measured with and without laser illumination on the $GaAs_{0.46}Sb_{0.54}$ device as shown in Fig. 1(c). The photoconductivity can then be depicted by the drain-source current difference between laser on and off, as illustrated in the Fig. 1(d). The photoconductivity can now be calculated as $\Delta\sigma_{\text{ph}} = \sigma_{\text{light}} - \sigma_{\text{dark}} \propto n_{\text{ph}}\mu_{\text{ph}}$, where n_{ph} is the photoinduced carrier density and μ_{ph} is the mobility of the excess holes. For $GaAs_{0.46}Sb_{0.54}$, as shown in Fig. 1(c), the photoinduced conductivity is almost a constant under different gate voltages, which indicates the constant value of $n_{\text{ph}}\mu_{\text{ph}}$. Thus, with application of the gate bias, neither the photoinduced carrier density nor the hole mobility contributes to the gate modulation of CPGE magnitude. As the spurious effects can be excluded by the photoinduced carrier transfer curves, the relation between Rashba SOC and gate voltage can therefore be obtained in the following gate-modulated CPGE results.

We now focus on the gate-voltage modulated CPGE results. The total electric field is a vector sum of the external field applied by the backgate, and the intrinsic surface electric field. Figure 4(a) shows the measured photocurrent of the $GaAs_{0.46}Sb_{0.54}$ nanowire device with $V_g = 0$, -10, -40, and -80 V, respectively. Figure 4(b) displays the deduced CPGE current with varying the gate voltage from $V_g = 30$

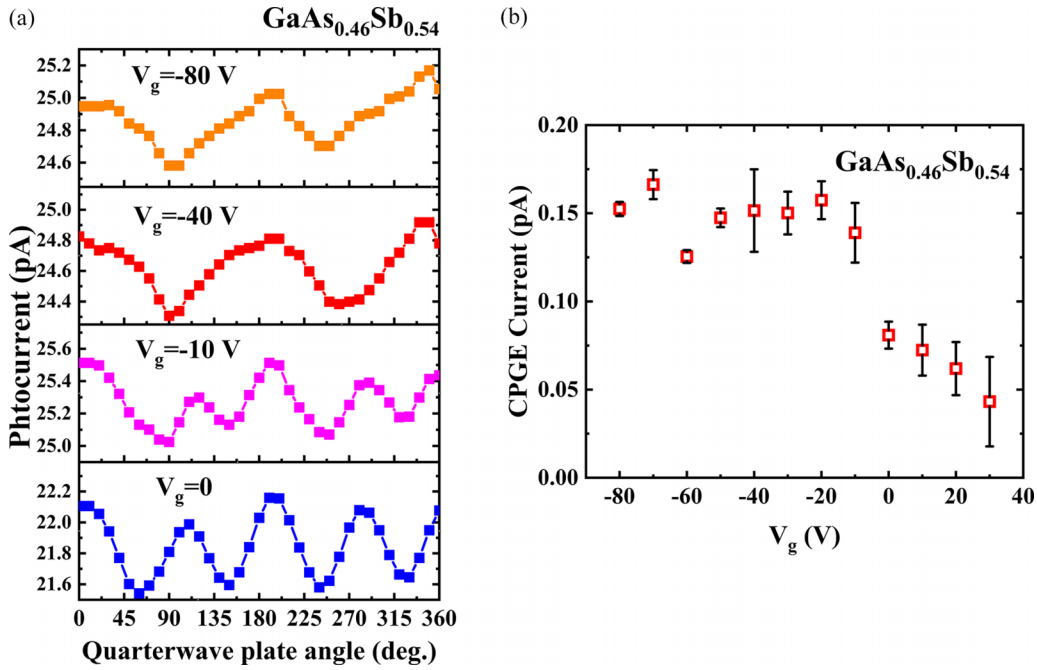

FIG. 4. (a) Raw data of $GaAs_{0.46}Sb_{0.54}$ nanowires at different gate voltages. (b) Extracted CPGE current as function of backgate voltage in $GaAs_{0.46}Sb_{0.54}$ nanowires, exhibiting transition from increasing to saturation as decreasing gate voltage.

to −80 V in a step of −10 V. Interestingly, we find that the CPGE current undergoes a sharp transition from increasing to saturation when varying the applied gate voltage. Specifically, as the gate voltage decreases from 30 to −10 V, the CPGE current rises sharply from 0.043 to 0.14 pA, and then increases to slightly above 0.15 pA as the gate voltage further decreases to −20 V. The relatively small CPGE current of 0.04 pA observed under a large positive gate voltage is attributed to the mutual cancellation between the gate electric field and the surface electric field. With application of the strong external electric field by the negative backgate, a 3.4× enhancement of the Rashba SOC for $GaAs_{0.46}Sb_{0.54}$ nanowire occurs. After that, the CPGE current fluctuates around this saturation value of about 0.15 pA along with a continuous decrease in the

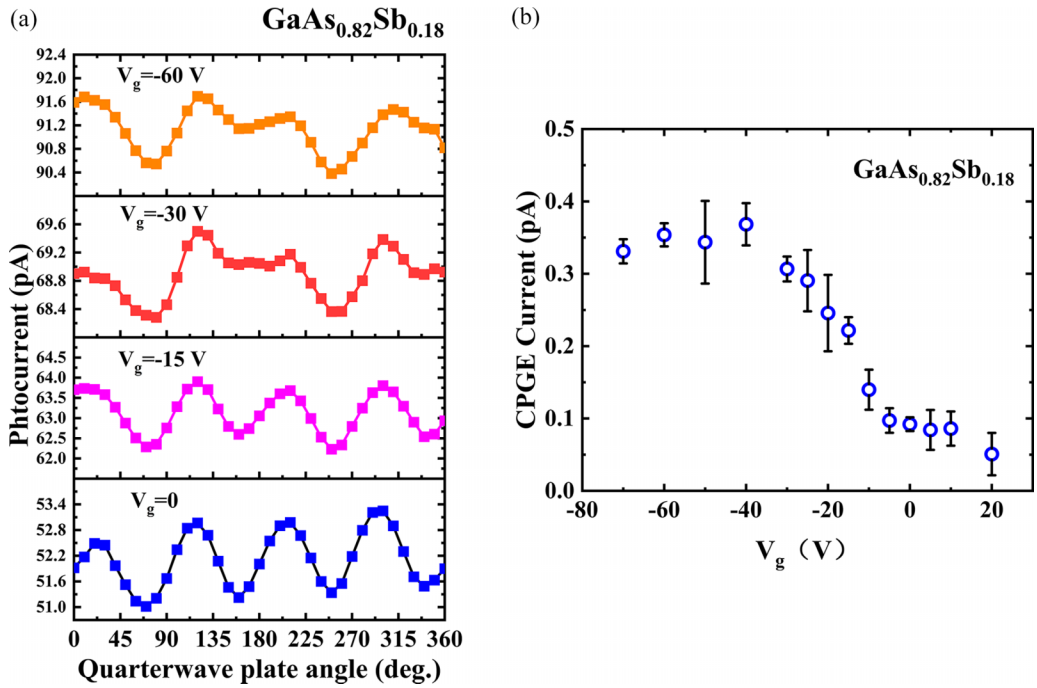

FIG. 5. (a) Raw data of CPGE measurements in $GaAs_{0.82}Sb_{0.18}$ nanowires at different gate voltages. (b) Extracted CPGE current as function of backgate voltage in $GaAs_{0.82}Sb_{0.18}$ nanowires. Transition from increasing to saturation also happens.

gate voltage. We infer that in the region of the positive gate voltage, the electric field induced by the gate is in the opposite direction with the field produced by the surface electric field. Hence, the total (net) electric field decreases, leading to the weakness in Rashba SOC and consequently in the CPGE current, with increase in the magnitude of a positive gate. On the other hand, under a negative gate bias, the induced electric field is in the same direction as that of the surface electric field. Therefore, the total electric field enhances with increase in the magnitude of the negative gate, causing the strength of the Rashba SOC, and, in turn, the amplitude of the CPGE current undergoes a transition from rapid increase to saturation with increase of the external electric field. This CPGE signature is consistent with the calculation results in Ref. [27], which confirms the detected Rashba SOC in the *p*-type nanowires is the predicted direct Rashba SOC. For the $GaAs_{0.82}Sb_{0.18}$ nanowire, the experimental result is similar: the amplitude of the CPGE current arises first and then saturates with decrease of the gate voltage, as seen in Fig. 5(a). As a result, the Rashba parameter α in $GaAs_{0.82}Sb_{0.18}$ nanowire also exhibits a transition from strong field dependence to saturation as shown in Fig. 5(b). Comparing with $GaAs_{0.46}Sb_{0.54}$, a bigger α enhancement of $4.1\times$ is obtained in the $GaAs_{0.82}Sb_{0.18}$ nanowire, which has a smaller radius, and the trend is consistent with theoretical calculation [27].

In conclusion, direct Rashba SOC of holes is observed in *p*-type semiconducting $GaAs_{1-x}Sb_x$ nanowires employing CPGE at room temperature. The CPGE current exhibits an increasing to saturation behavior with decrease of the gate voltage, indicating that the Rashba SOC parameter undergoes a transition from being field dependent to saturation with increasing the magnitude of the electric field, in contrast to the *n*-type semiconducting nanowires. These results are consistent with the predictions presented in Ref. [27]. By offering the experimental signature of the direct Rashba SOC of holes, we may pave an alternative way for manipulating spins, which is essential for future applications in spintronics.

This work was supported by the National Key Research and Development Program of China (Grants No. 2022YFB3605604 and No. 2018YFE0125700) and the National Natural Science Foundation of China (Grants No. 62225402, No. 61927806, No. 62234001, and No. U22A2074).

[1] V. Mourik, K. Zuo, S. M. Frolov, S. R. Plissard, E. P. A. M. Bakkers, and L. P. Kouwenhoven, Signatures of Majorana fermions in hybrid superconductor-semiconductor nanowire devices, Science **336**, 1003 (2012).

[2] A. Das, Y. Ronen, Y. Most, Y. Oreg, M. Heiblum, and H. Shtrikman, Zero-bias peaks and splitting in an Al-InAs nanowire topological superconductor as a signature of Majorana fermions, Nat. Phys. **8**, 887 (2012).

[3] J. D. Sau, R. M. Lutchyn, S. Tewari, and S. Das Sarma, Generic New Platform for Topological Quantum Computation Using Semiconductor Heterostructures, Phys. Rev. Lett. **104**, 040502 (2010).

[4] M. Z. Hasan and C. L. Kane, Colloquium: Topological insulators, Rev. Mod. Phys. **82**, 3045 (2010).

[5] X.-L. Qi and S.-C. Zhang, Topological insulators and superconductors, Rev. Mod. Phys. **83**, 1057 (2011).

[6] J. E. Moore, The birth of topological insulators, Nature (London) **464**, 194 (2010).

[7] S. M. Frolov, S. R. Plissard, S. Nadj-Perge, L. P. Kouwenhoven, and E. P. A. M. Bakkers, Quantum computing based on semiconductor nanowires, MRS Bull. **38**, 809 (2013).

[8] S. Nadj-Perge, S. M. Frolov, E. P. A. M. Bakkers, and L. P. Kouwenhoven, Spin-orbit qubit in a semiconductor nanowire, Nature (London) **468**, 1084 (2010).

[9] I. Zutic, J. Fabian, and S. Das Sarma, Spintronics: Fundamentals and applications, Rev. Mod. Phys. **76**, 323 (2004).

[10] D. D. Awschalom and M. E. Flatte, Challenges for semiconductor spintronics, Nat. Phys. **3**, 153 (2007).

[11] A. Manchon, H. C. Koo, J. Nitta, S. M. Frolov, and R. A. Duine, New perspectives for Rashba spin-orbit coupling, Nat. Mater. **14**, 871 (2015).

[12] J. Nitta, T. Akazaki, H. Takayanagi, and T. Enoki, Gate Control of Spin-Orbit Interaction in an Inverted $In_{0.53}Ga_{0.47}As/In_{0.52}Al_{0.48}As$ Heterostructure, Phys. Rev. Lett. **78**, 1335 (1997).

[13] M. Schultz, F. Heinrichs, U. Merkt, T. Colin, T. Skauli, and S. Lovold, Rashba spin splitting in a gated HgTe quantum well, Semicond. Sci. and Technol. **11**, 1168 (1996).

[14] S. Datta and B. Das, Electronic analog of the electrooptic modulator, Appl. Phys. Lett. **56**, 665 (1990).

[15] H. C. Koo, J. H. Kwon, J. Eom, J. Chang, S. H. Han, and M. Johnson, Control of spin precession in a spin-injected field effect transistor, Science **325**, 1515 (2009).

[16] Y. Kanai, R. S. Deacon, S. Takahashi, A. Oiwa, K. Yoshida, K. Shibata, K. Hirakawa, Y. Tokura, and S. Tarucha, Electrically tuned spin-orbit interaction in an InAs self-assembled quantum dot, Nat. Nanotechnol. **6**, 511 (2011).

[17] R. Yang, K. H. Gao, Y. H. Zhang, P. P. Chen, G. Yu, L. M. Wei, T. Lin, N. Dai, and J. H. Chu, Weak field magnetoresistance of narrow-gap semiconductor InSb, J. Appl. Phys. **109**, 063703 (2011).

[18] R. Jansen, Silicon spintronics, Nat. Mater. **11**, 400 (2012).

[19] K. Ishizaka, M. S. Bahramy, H. Murakawa, M. Sakano, T. Shimojima, T. Sonobe, K. Koizumi, S. Shin, H. Miyahara, A. Kimura, K. Miyamoto, T. Okuda, H. Namatame, M. Taniguchi, R. Arita, N. Nagaosa, K. Kobayashi, Y. Murakami, R. Kumai, Y. Kaneko, Y. Onose, and Y. Tokura, Giant Rashba-type spin splitting in bulk BiTeI, Nat. Mater. **10**, 521 (2011).

[20] D. Di Sante, P. Barone, R. Bertacco, and S. Picozzi, Electric control of the giant Rashba effect in bulk GeTe, Adv. Mater. **25**, 509 (2013).

[21] M. Liebmann, C. Rinaldi, D. Di Sante, J. Kellner, C. Pauly, R. N. Wang, J. E. Boschker, A. Giussani, S. Bertoli, M. Cantoni, L. Baldrati, M. Asa, I. Vobornik, G. Panaccione, D. Marchenko, J. Sanchez-Barriga, O. Rader, R. Calarco, S. Picozzi, R. Bertacco, and M. Morgenstern, Giant Rashba-type spin splitting in ferroelectric GeTe(111), Adv. Mater. **28**, 560 (2016).

[22] Y. Hu, F. Kuemmeth, C. M. Lieber, and C. M. Marcus, Hole spin relaxation in Ge-Si core-shell nanowire qubits, Nat. Nanotechnol. **7**, 47 (2011).

[23] R. J. Warburton, Single spins in self-assembled quantum dots, Nat. Mater. **12**, 483 (2013).

[24] R. Winkler, *Spin-Orbit Coupling Effects in Two-Dimensional Electron and Hole Systems*, Springer Tracts in Modern Physics Vol. 191 (Springer, New York, 2003).

[25] R. Moriya, K. Sawano, Y. Hoshi, S. Masubuchi, Y. Shiraki,A. Wild, C. Neumann, G. Abstreiter, D. Bougeard, T. Koga, and T. Machida, Cubic Rashba Spin-Orbit Interaction of a Two-Dimensional Hole Gas in a Strained-Ge/SiGe Quantum Well, Phys. Rev. Lett. **113**, 086601 (2014).

[26] C. Kloeffel, M. Trif, and D. Loss, Strong spin-orbit interaction and helical hole states in Ge/Si nanowires, Phys. Rev. B **84**, 195314 (2011).

[27] J.-W. Luo, S.-S. Li, and A. Zunger, Rapid Transition of the Hole Rashba Effect from Strong Field Dependence to Saturation in Semiconductor Nanowires, Phys. Rev. Lett. **119**, 126401 (2017).

[28] J.-W. Luo, L. Zhang, and A. Zunger, Absence of intrinsic spin splitting in one-dimensional quantum wires of tetrahedral semiconductors, Phys. Rev. B **84**, 121303 (2011).

[29] L. Li, D. Pan, Y. Xue, X. Wang, M. Lin, D. Su, Q. Zhang, X. Yu, H. So, D. Wei, B. Sun, P. Tan, A. Pan, and J. Zhao, Near full-composition-range high-quality $GaAs_{1-x}Sb_x$ nanowires grown by molecular-beam epitaxy, Nano Lett. **17**, 622 (2017).

[30] S. D. Ganichev and W. Prettl, Spin photocurrents in quantum wells, J. Phys.: Condens. Matter **15**, R935 (2003).

[31] H. Guan, N. Tang, X. Xu, L. Shang, W. Huang, L. Fu, X. Fang, J. Yu, C. Zhang, X. Zhang, L. Dai, Y. Chen, W. Ge, and B. Shen, Photon wavelength dependent valley photocurrent in multilayer MoS_2, Phys. Rev. B **96**, 241304 (2017).

[32] H. Yuan, X. Wang, B. Lian, H. Zhang, X. Fang, B. Shen, G. Xu, Y. Xu, S.-C. Zhang, H. Y. Hwang, and Y. Cui, Generation and electric control of spin-valley-coupled circular photogalvanic current in WSe_2, Nat. Nanotechnol. **9**, 851 (2014).

[33] C. Yin, H. Yuan, X. Wang, S. Liu, S. Zhang, N. Tang, F. Xu, Z. Chen, H. Shimotani, Y. Iwasa, Y. Chen, W. Ge, and B. Shen, Tunable surface electron spin splitting with electric double-layer transistors based on InN, Nano Lett. **13**, 2024 (2013).

[34] J. Duan, N. Tang, X. He, Y. Yan, S. Zhang, X. Qin, X. Wang, X. Yang, F. Xu, Y. Chen, W. Ge, and B. Shen, Identification of helicity-dependent photocurrents from topological surface states in Bi_2Se_3 gated by ionic liquid, Sci. Rep. **4**, 4889 (2014).

[35] J. Yu, X. Zeng, L. Zhang, K. He, S. Cheng, Y. Lai, W. Huang, Y. Chen, C. Yin, and Q. Xue, Photoinduced inverse spin Hall effect of surface states in the topological insulator Bi_2Se_3, Nano Lett. **17**, 7878 (2017).

[36] H. Guan, N. Tang, H. Huang, X. Zhang, M. Su, X. Liu, L. Liao, W. Ge, and B. Shen, Inversion symmetry breaking induced valley Hall effect in multilayer WSe_2, ACS Nano **13**, 9325 (2019).

[37] S. Zhang, N. Tang, W. Jin, J. Duan, X. He, X. Rong, C. He, L. Zhang, X. Qin, L. Dai, Y. Chen, W. Ge, and B. Shen, Generation of Rashba spin-orbit coupling in CdSe nanowire by ionic liquid gate, Nano Lett. **15**, 1152 (2015).

[38] K. F. Mak, K. L. McGill, J. Park, and P. L. McEuen, The valley Hall effect in MoS_2 transistors, Science **344**, 1489 (2014).